

Why urban heterogeneity limits the 15-minute city

Marc Barthelemy^{1,2,3,*}

¹Université Paris-Saclay, CNRS, CEA, Institut de Physique Théorique, 91191 Gif-sur-Yvette, France

²Centre d'Analyse et de Mathématique Sociales (CNRS/EHESS), Paris, France

³Complexity Science Hub, Vienna, Austria

(Dated: March 13, 2026)

The “15-minute city” has emerged as a central paradigm in urban planning, promoting universal access to work and essential services within short travel times. Its feasibility—particularly for commuting to work—has however rarely been examined quantitatively. Here, we show that proximity to employment is fundamentally constrained by the internal structure of urban economies. Combining urban geometry with empirically observed firm-size distributions, we derive a lower bound on commuting times that holds independently of planning choices or transport technologies. This bound reveals a sharp transition: when employment is sufficiently concentrated, no spatial rearrangement of workplaces can ensure uniformly short commutes, even under optimal placement. Applied to Paris and its near suburbs, we find that achieving universal 15-minute commutes would require substantial economic restructuring or differentiated mobility strategies. The relevant question is therefore not whether an x -minute city is achievable, but what the minimal feasible x is given a city’s economic structure and spatial scale.

MAIN

Building on earlier traditions of neighborhood-based urbanism and accessibility planning, the “15-minute city” [1] (or more generally the x -minute city) promotes the idea that essential urban functions—work, commerce, healthcare, and education—should be reachable within a short travel time from one’s residence, ideally by walking or cycling. Initially framed as a response to climate change, social inequalities, and car-dependent urban growth, it has rapidly gained visibility as a normative model for sustainable urban development [2], promising reduced car dependence and emissions alongside improvements in quality of life, public health, and social inclusion [3].

Although employment is explicitly included in the original formulation [1], it has proven difficult to operationalize empirically, and commuting-to-work constraints have received limited quantitative attention. Concerns about job–housing proximity are longstanding: classic work on accessibility and job–housing balance already showed that residences in job-rich areas are associated with shorter commutes [4]. The 15-minute city can thus be viewed as a strengthening of this principle, aiming not merely at average reductions in commuting time but at universal proximity for all workers. Recent empirical work, however, shows that proximity to services does not necessarily translate into localized travel, particularly for work trips [5].

Methodological reviews confirm this gap between conceptual ambition and empirical practice, showing that the 15-minute city lacks a unified operational definition, relies on heterogeneous indicators, and predominantly measures access to local services, while commut-

ing responds more weakly to proximity-based interventions [6–12]. Large-scale empirical assessments further quantify substantial heterogeneity of accessibility within and across cities worldwide, highlighting the role of population density and resource distribution in shaping proximity outcomes [6, 7, 13]. Despite these advances, the feasibility of the x -minute city remains poorly understood at a more fundamental level. In particular, recent reviews [6, 7] make clear that most studies stop short of addressing a structural question: whether universal proximity to work is achievable *in principle*, independently of specific planning choices, service redistribution strategies, or mobility technologies.

In particular, Bruno et al. [13] propose a global framework to quantify accessibility to essential services and to simulate their optimal redistribution across cities worldwide. They measure proximity times to nine categories of point-of-interests (outdoor activities, learning, supplies, eating, moving, cultural activities, physical exercise, services, and healthcare), and develop an algorithm to relocate these amenities so as to equalise services per capita and increase the fraction of the population living within a 15-minute condition. Their results highlight strong heterogeneity across cities and show that substantial service redistribution would be required in many urban contexts. However, the most significant structural obstacle to achieving a universal 15-minute city lies in commuting to work. Unlike local amenities such as shops or schools, employment is intrinsically heterogeneous: a small number of large firms employ a substantial fraction of the workforce, while many small establishments coexist alongside them. Crucially, employment is not a freely replicable service that can be redistributed without altering the underlying economic structure itself. This difference is therefore not merely quantitative but structural.

More precisely, firm sizes follow broad, approximately Zipfian distributions across countries, sectors, and time periods [14–18]. Although firm-level employment data

* marc.barthelemy@ipht.fr

are typically available only in aggregated form at the urban scale, establishment counts reveal substantial within-city heterogeneity, with large employers accounting for a disproportionate share of employment (see section I of the SI). In general, we can expect that large metropolitan areas necessarily host the upper tail of the firm-size distribution [19], making economic heterogeneity a structural constraint at the urban scale.

This observation raises a fundamental question left open by existing studies [6, 7]: under what conditions is it possible, even in principle, to locate firms in space such that every worker can reach their workplace within a prescribed travel time τ_0 ? We address this question using a minimal spatial framework combining three ingredients: (i) a population distributed over a city of area A , (ii) firms whose sizes follow a Zipf distribution with exponent γ , and (iii) an optimization problem in which firm locations are chosen to minimize the maximum commuting distance. This framework yields strict theoretical bounds on proximity, which we confront with numerical optimization and a case study of Paris and its near suburbs.

MODEL

To isolate the role of the journey-to-work commute, we introduce a minimal model that focuses on this single ingredient and reveals the existence of a structural lower bound on commuting time. We thus consider an idealized city of characteristic radius R (typically of order $\sqrt{A/\pi}$, where A is the urban area), and total employment E . Residents are assumed to be uniformly distributed in space unless stated otherwise. Employment is provided by N firms whose sizes are heterogeneous and ranked by decreasing employment $m_1 > m_2 > \dots > m_N$. Firm sizes are assumed to follow a Zipf distribution, such that the firm of rank r employs $m_r \propto r^{-\gamma}$ workers, where the exponent γ controls the degree of economic inequality: $\gamma = 0$ corresponds to homogeneous firms, while larger values of γ indicate increasingly concentrated employment in a small number of large firms.

The framework is intentionally minimal and aims to identify feasibility constraints that are independent of detailed urban design, land-use regulation, or transport technologies. It applies most directly at spatial scales where employment locations compete for access to the same pool of residents, such as neighborhoods, districts, or central urban areas. At larger metropolitan scales, many cities exhibit a polycentric organization with multiple employment centers rather than a single dominant core [20–24]. In such cases, proximity constraints should be evaluated at the level of individual subcenters rather than across the entire metropolitan area. Applying a 15-minute constraint at the metropolitan scale is therefore not meaningful in general, as commuting distances necessarily exceed this threshold even under optimistic mobility assumptions. Thus, proximity-based planning

implicitly assumes a decomposition of cities into smaller functional units, and the present framework provides a feasibility test for such units.

The normalization condition $\sum_{r=1}^N m_r = E$, together with $m_r = m_1 r^{-\gamma}$, fixes the size of the largest firm as

$$m_1 = \frac{E}{H_N(\gamma)}, \quad (1)$$

where $H_N(\gamma) = \sum_{r=1}^N r^{-\gamma}$ is the n -th generalized harmonic number. For large N , $H_N(\gamma) \sim N^{1-\gamma}/(1-\gamma)$ for $\gamma < 1$, $H_N(1) \sim \log N$ in the marginal case, and $H_N(\gamma) \rightarrow \zeta(\gamma)$ for $\gamma > 1$, where $\zeta(\gamma)$ denotes the Riemann zeta function. This result Eq. 1 shows that the firm-size distribution alone determines how many workers must be served by the largest employer, independently of spatial considerations.

Each worker is assigned to a single firm, and commuting is approximated by straight-line (Euclidean) distances, a standard first-order approximation in urban spatial models [25], which captures the underlying spatial constraint independently of network details. For a given spatial arrangement of firms, we define ℓ_{\max} as the maximum commuting distance across the population. The central feasibility question is whether firms can be located in space such that $\ell_{\max} \leq L_0$, where L_0 denotes a prescribed maximum commuting distance (or, equivalently, a maximum commuting time). Geometrically, the worker–firm assignment problem is equivalent to a weighted Voronoi partition [26], in which firm sizes act as weights constraining the spatial extent of their catchment areas. As firm-size heterogeneity increases, these weighted cells become increasingly distorted, forcing some regions to span large distances and driving the proximity feasibility transition.

RESULTS

Theoretical feasibility constraints

We derive a strict theoretical constraint on the feasibility of an x -minute city that holds independently of any numerical optimization. This constraint follows from elementary geometric considerations combined with firm-size heterogeneity and defines an absolute lower bound that no spatial rearrangement of workplaces can overcome.

The main idea is that the dominant constraint is imposed by the largest firm. Assuming that firm sizes follow a Zipf distribution with exponent γ , the largest firm employs a fraction of the total workforce given by Eq. 1. Even if this firm is optimally located at the point of maximum population density, it must recruit its workforce from a finite catchment area which has a certain size. For a uniform worker density $\rho = E/A$, the radius ℓ_{\max} of this catchment area satisfies $\rho\pi\ell_{\max}^2 = m_1$. Requiring that all workers commute less than a prescribed distance

L_0 therefore yields the lower bound

$$L_0 \geq L_0^* \equiv \sqrt{\frac{A/\pi}{H_N(\gamma)}}. \quad (2)$$

In the numerical model on a disk of radius R , this reduces to $L_0/R \geq 1/\sqrt{H_N(\gamma)}$. Expressed in terms of time rather than distance, the minimal commuting time achievable in this city is then

$$\tau_0(\gamma) = \frac{1}{v} \frac{\sqrt{A/\pi}}{\sqrt{H_N(\gamma)}}, \quad (3)$$

where v is the characteristic travel speed (walking or biking). Equation (3) constitutes a fundamental limit on urban proximity: it cannot be improved by redistributing firms, modifying transport infrastructure, or altering land-use patterns. It provides the reference against which numerical optimizations and empirical case studies are interpreted below (more details and discussion can be found in section II of the SI).

The factor $\sqrt{A/\pi}/v$ corresponds to the time required to traverse the city radius, while the effect of firm-size heterogeneity enters through the denominator $\sqrt{H_N(\gamma)}$. The resulting constraint depends qualitatively on the value of γ . For $\gamma > 1$, the harmonic number converges to $H_N(\gamma) \rightarrow \zeta(\gamma)$ in the large- N limit, yielding a finite asymptotic lower bound $L_0^* = \sqrt{A/\pi}/\sqrt{\zeta(\gamma)}$. In this regime, increasing the number of firms cannot reduce commuting distances below a fixed fraction of the city size, revealing a structural obstruction to universal short commutes. By contrast, in the homogeneous limit $\gamma = 0$, one has $H_N(0) = N$ and the bound reduces to the purely geometric scaling $L_0^* = \sqrt{A/\pi}/\sqrt{N}$, which can be made arbitrarily small by increasing the number of firms.

The transition between these regimes reflects a qualitative change in the nature of proximity constraints, from geometry-dominated at low heterogeneity to extreme-value-dominated at large γ . Empirically, estimates based on binned establishment-size data for U.S. metropolitan areas yield values in the range $\gamma \in [0.4, 1.0]$, with mean $\langle \gamma \rangle \simeq 0.71 \pm 0.12$ (see the section I of the SI). For the Paris metropolitan area, available data are consistent with a larger exponent, $\gamma \simeq 1.4$ (see section V of the SI), placing it deep in the high-heterogeneity regime where proximity constraints become intrinsically difficult to satisfy at the metropolitan scale.

Numerical phase diagram

We next examine how the theoretical feasibility bounds manifest at finite system size using explicit spatial optimization. The aim of this numerical analysis is not to calibrate real cities, but to probe the robustness and sharpness of the feasibility constraint with finite numbers of workers and firms.

For fixed values of (γ, E, N) and a prescribed capacity tolerance δ , firm locations are optimized using simulated annealing [27] to minimize the maximum commuting distance ℓ_{\max} . The tolerance δ quantifies the allowed mismatch between firm capacity and the number of workers assigned to it: a firm of size m can accommodate a number of workers in the interval $[(1 - \delta)m, (1 + \delta)m]$. This parameter captures realistic flexibility in firm capacity, congestion effects, and imperfect matching between workers and establishments. As derived in Section III of the SI, capacity flexibility modifies the theoretical lower bound by replacing the factor $1/H_N(\gamma)$ with $(1 - \delta)/H_N(\gamma)$, yielding a reduced minimum commuting time $\tau_{\min}(\gamma, \delta) = \tau_{\min}(\gamma, 0) \sqrt{1 - \delta}$. The optimization is repeated over multiple independent realizations of the population distribution to estimate both the mean optimal ℓ_{\max} and its fluctuations (for more details on the numerical simulation, see the section IV in the SI). Throughout this analysis, we assume that the number of establishments scales proportionally with total employment, $N \simeq \alpha E$, following empirical observations for U.S. Metropolitan Statistical Areas, with $\alpha \simeq 0.06$. This assumption fixes the average firm size, $\langle m \rangle = 1/\alpha$, and closes the model (see the SI).

We show in Fig. 1 the result of the optimization for a representative example with $E = 1000$ employees and $N = 60$ firms, with firm sizes distributed according to a Zipf law with exponent $\gamma = 1.5$. Starting from a random spatial configuration of firms and a random allocation of workers to firms, the simulated annealing algorithm searches for the arrangement that minimizes the maximal commuting distance ℓ_{\max} . In the initial configuration, the maximal commute is $\ell_{\max} = 1.68$, which is close to the diameter 2 of the disk. After optimization, the maximal commuting distance decreases to $\ell_{\max} \approx 0.70$, corresponding to roughly one quarter of the system diameter. The optimized configuration exhibits a clear spatial organization: the largest firm is located near the center of the system, while smaller firms are distributed toward the periphery. This arrangement minimizes extreme commuting distances and prevents the occurrence of very long trips.

The previous example illustrates how spatial optimization reduces extreme commuting distances in a single configuration. We now examine how this limit depends on the degree of economic heterogeneity. Figure 2 shows the optimized maximal commuting distance ℓ_{\max} as a function of the firm-size exponent γ , together with the theoretical lower bound L_0^* . Two main results emerge. First, the numerical solutions reproduce the qualitative trend predicted by the theory: increasing firm-size heterogeneity leads to a monotonic increase in the minimal achievable commuting distance. The transition from feasible to infeasible proximity regimes is sharp, confirming that heterogeneity acts as the dominant control parameter. Second, the optimized configurations lie systematically above the theoretical bound. This offset reflects finite-size effects and the discrete nature of the spatial

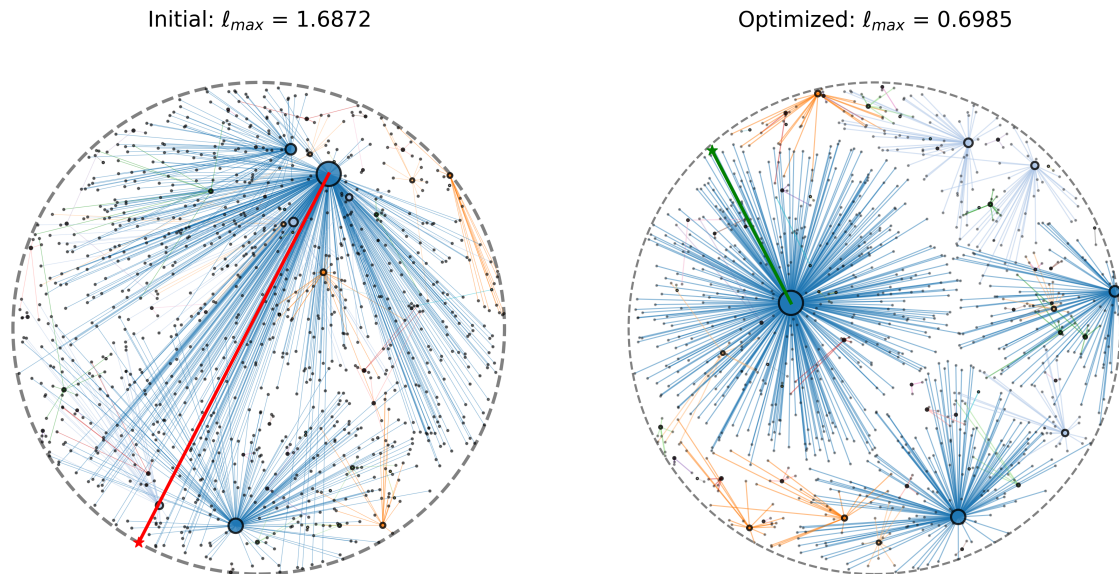


FIG. 1. **Comparison before and after optimization.** Illustration of the simulated annealing optimization for a representative example ($E = 1000$, $N = 60$, $\gamma = 1.5$, $m_1 = 424.6$, $m_N = 1$). Firm locations are initially assigned at random (symbol size proportional to firm size), and workers are randomly allocated to firms. The initial configuration yields a maximal commuting distance $\ell_{\max} \approx 1.69$. After simulated annealing ($T_{\text{init}} = 0.5$, $T_{\text{min}} = 10^{-4}$, $\alpha = 0.95$, $n_{\text{steps}} = 1000$ per temperature), the system converges to an optimized spatial arrangement with $\ell_{\max} \approx 0.70$, corresponding to a reduction of $\sim 60\%$. In the optimized configuration, the largest firms are located closer to the center of the system, which reduces extreme commuting distances and prevents the occurrence of very long trips.

optimization problem. While the analytical results provide asymptotic lower bounds valid in the limit of large populations, numerical realizations involve finite numbers of firms and residents. These finite-size constraints prevent the numerical solutions from reaching the theoretical bound, creating a systematic gap above it. The theoretical curve therefore acts as a strict lower bound, while the numerical results represent realizable configurations at moderate system size.

The discrepancy between numerical and theoretical bounds is largest around and above $\gamma \simeq 1$, a range consistent with empirically observed Zipf-like firm-size distributions. This value marks a qualitative crossover between weakly and strongly heterogeneous regimes. For $\gamma > 1$, firm sizes span several orders of magnitude without a characteristic scale, and the optimization becomes dominated by a small number of extreme firms. In this regime, ℓ_{\max} is controlled by rare, system-spanning constraints rather than by typical firms, leading to an abrupt breakdown of proximity.

Overall, these numerical results show that the infeasibility transition predicted by the theory is already visible at moderate system sizes. In finite systems, proximity constraints are even stronger: the optimized maximum commuting distance is systematically larger than the theoretical lower bound.

Paris as a stress test for the 15-minute city

Paris provides a particularly challenging case for the feasibility of a 15-minute city. Approximately 1.8 million individuals work inside the city of Paris, but commuting flows are highly asymmetric: nearly 60% (1,080,000 individuals) of workers employed in Paris reside outside the city (data for 2017; [28]). Among these 1.08 million workers, about 55% come from the near suburbs (the *petite couronne*), with the remainder residing in more distant suburbs and other regions. We therefore focus on the 1.314 million individuals who work in Paris and live either in Paris or in its near suburbs, excluding the outer suburbs (the *grande couronne*), where commuting distances typically exceed 20 km and a 15-minute constraint is unrealistic.

Paris hosts approximately 406 000 establishments [29], corresponding to an average firm size of $\langle m \rangle \simeq 4.4$ employees. Rather than relying on a single estimate of N for the combined area of Paris and the *petite couronne* (which for example would be $\sim 3 \times 10^5$ for 4.4 employees per firm), we vary N over almost two orders of magnitude, from 10^4 to 5×10^5 , encompassing any plausible value. To characterize firm-size heterogeneity, we estimate the Zipf exponent γ using establishment-size data available at the scale of the Paris urban area. Using INSEE data for 2023 [30], we obtain a relatively large value $\gamma \simeq 1.38$, indicating strong employment concentration.

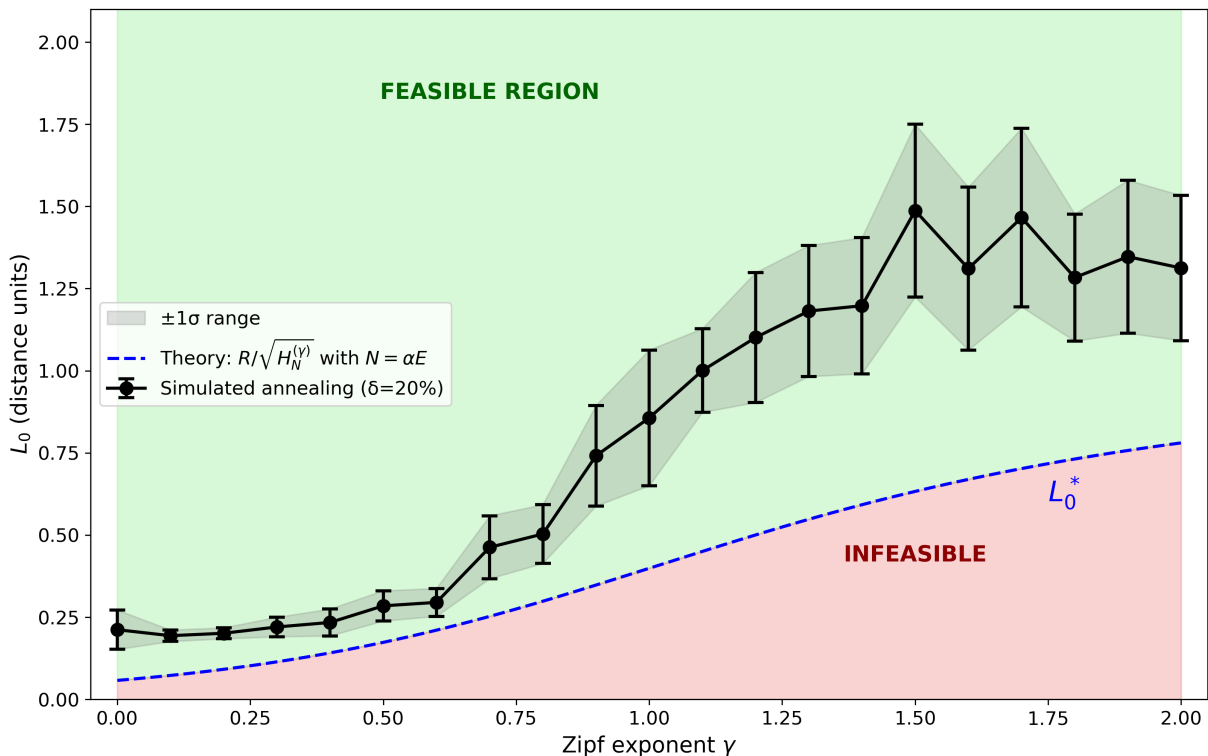


FIG. 2. **Finite-size phase diagram of proximity feasibility.** Optimized maximum commuting distance ℓ_{\max} as a function of the firm-size exponent γ , obtained from simulated annealing for a system with total employment $E = 5000$, city radius $R = 1$, establishment density $N = \alpha E$ with $\alpha = 0.06$, and capacity tolerance $\delta = 20\%$. Symbols show averages over 10 independent spatial configurations. The dashed line indicates the theoretical lower bound L_0^* given by Eq. 2 for a uniform population density. Green and red shaded regions denote, respectively, feasible and infeasible proximity regimes: below the bound, no spatial arrangement of establishments can achieve a smaller maximum commuting distance, whereas above it realizable configurations exist.

Given uncertainties in the estimation, we treat γ as a control parameter and explore a broad range of values.

The central question is whether these N (with $N \in [10^4, 5 \times 10^5]$) establishments can be spatially reorganized over Paris and the *petite couronne* such that all 1.314 million workers commute less than 15 minutes. To address this question, we use the theoretical lower bound $\tau_{\min}(\gamma)$ derived above. At this scale, population density can be reasonably approximated as uniform, allowing direct application of the analytical framework.

Figure 3 shows the resulting minimal commuting time $\tau_0(\gamma)$ as a function of firm-size heterogeneity for both walking and cycling, across a wide range of establishment counts N . Two main regimes emerge. For $\gamma \gtrsim 1$, the curves at different N collapse onto a single line: in this regime $H_N(\gamma)$ is well approximated by $\zeta(\gamma)$, and the theoretical bound depends only on the area and the exponent, not on the number of firms. For $\gamma \lesssim 1$, by contrast, $H_N(\gamma)$ grows without bound with N , making τ_0 sensitive to the precise establishment count; larger N spreads workers across more, smaller catchment areas and thereby reduces the worst-case commuting distance. For Paris, the empirical firm-size distribution, however, falls in the $\gamma > 1$ regime, where the bound

is N -independent. The shaded bands quantify the additional gain from capacity flexibility δ . The multiplicative reduction $\sqrt{1-\delta}$ is independent of γ (see SI), but even for $\delta = 0.3$ —corresponding to a roughly 16% decrease in τ_0 —the correction is far too modest to bring commuting times below the 15-minute threshold for any empirically relevant value of γ . Crucially, these results show that for a wide range of γ values compatible with empirical estimates, including $\hat{\gamma} \simeq 1.38$, the 15-minute threshold cannot be reached—neither by increasing the number of establishments, nor by allowing substantial capacity flexibility. While increasing travel speed through cycling significantly reduces commuting times, it is generally insufficient to offset the constraint imposed by firm-size heterogeneity. These results indicate that, at the scale of Paris and its near suburbs, achieving a 15-minute city would require not only improvements in mobility but a substantial reorganisation of economic activity itself.

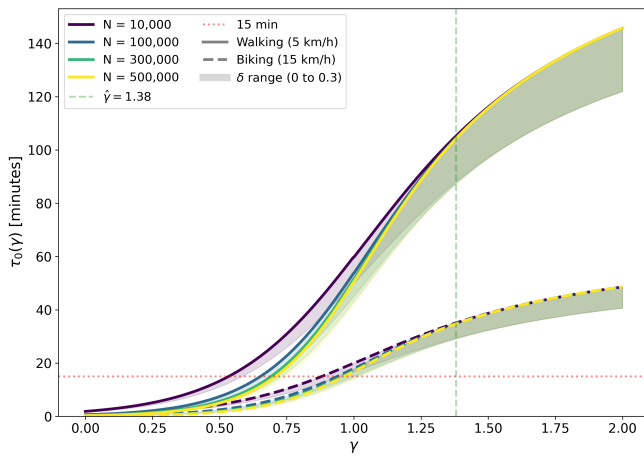


FIG. 3. **Theoretical minimum commuting time for Paris and its near suburbs.** Minimal achievable commuting time $\tau_0(\gamma)$ as a function of the firm-size exponent γ , computed for the combined area of Paris and the *petite couronne* ($A = 762 \text{ km}^2$). Solid curves correspond to walking ($v = 5 \text{ km/h}$) and dashed curves to cycling ($v = 15 \text{ km/h}$); colour encodes the number of establishments N_{est} , with values 10^3 , 10^4 , 10^5 , 3×10^5 , and 5×10^5 . The shaded band beneath each curve shows the reduction in τ_0 afforded by a capacity flexibility δ ranging from 0 (upper edge) to 0.3 (lower edge), corresponding to a multiplicative factor $\sqrt{1 - \delta}$. The horizontal dotted line marks the 15-minute threshold, while the vertical dashed line indicates the empirical estimate $\hat{\gamma} \simeq 1.38$.

STRUCTURAL LIMITS TO URBAN PROXIMITY

Our results reveal a fundamental limitation of proximity-based urban ideals that arises from economic organization rather than from urban form or transport infrastructure. The key mechanism limiting proximity discussed here is firm-size heterogeneity. When employment is broadly distributed and includes very large establishments, a small number of firms must draw workers from spatially extended catchment areas to satisfy their capacity. These dominant employers therefore impose long commuting distances, even under optimal spatial placement. By contrast, when firms are relatively homogeneous and remain small, employment can be organized through many local catchment areas, allowing commuting distances to remain short throughout the city.

Firm-size heterogeneity is a robust empirical feature

of modern economies and is likely to remain significant within cities, although more detailed urban-scale data are needed to quantify it precisely. If the Paris metropolitan area is representative, many large cities may lie deep in the heterogeneous regime identified here, where the theoretical lower bound on commuting time is already large. In this regime, short commutes for all workers cannot, in principle, be ensured solely through spatial reorganization, even under optimistic assumptions about travel speeds. This implies that the 15-minute city is not universally achievable, but depends on the specific economic and spatial characteristics of each city. While firm-size heterogeneity is a central ingredient of the present analysis, it is not the only factor shaping commuting patterns and accessibility. The purpose of this work is not to provide an exhaustive description of urban complexity, but to identify fundamental theoretical constraints that apply independently of particular planning choices.

Importantly, the framework developed here also offers a practical way to estimate the minimum achievable proximity time in a given city. When empirical data are available for the firm-size distribution (through γ , N , and E) and for the spatial extent A of the urban area, the theory yields a lower bound on commuting time that no spatial rearrangement of workplaces alone can overcome. In this sense, the relevant question is not whether a city can be made into an “ x -minute city” for a prescribed value of x , but rather what the smallest feasible x is, given its economic structure and geometry. This perspective suggests a differentiated strategy: proximity-based planning may successfully ensure local access to daily amenities, while access to employment in heterogeneous urban economies may require complementary mobility solutions and efficient transport networks rather than purely spatial redistribution. By quantifying these structural limits, this work provides a framework for evaluating where and when proximity-based urban planning can realistically succeed.

Acknowledgments: I thank Jieun Lee and Chris Webster for interesting discussions on the 15 minute city.

Data availability statement: The datasets used in this study are freely available from public repositories: [28–31].

Competing interests: None.

-
- [1] C. Moreno, Z. Allam, D. Chabaud, C. Gall, and F. Pratlong, “Introducing the “15-minute city”: Sustainability, resilience and place identity in future post-pandemic cities,” *Smart Cities*, vol. 4, pp. 93–111, 2021.
 - [2] C. Moreno, D. Chabaud, and C. Gall, “The 15-minute city model: An integrated urban approach and a game changing lifestyle narrative,” in *From the City as a*

Project to the City Project: Volume II: The 21st Century. Cham: Springer Nature Switzerland, 2025, pp. 681–707.

- [3] B. E. Saelens, J. F. Sallis, and L. D. Frank, “Environmental correlates of walking and cycling: Findings from the transportation, urban design, and planning literatures,” *Annals of Behavioral Medicine*, vol. 25, 2003.

- [4] D. M. Levinson, “Accessibility and the journey to work,” *Journal of Transport Geography*, vol. 6, pp. 11–21, 1998.
- [5] X. Zhang, A. Poliakov, H. Tenkanen, and E. Arcaute, “Recurrent visitations expose the paradox of human mobility in the 15-minute city vision,” *arXiv preprint*, 2025.
- [6] B. Büttner, C. Silva, L. Merlin, and K. T. Geurs, “Just around the corner: Accessibility by proximity in the 15-minute city,” *Journal of Urban Mobility*, vol. 6, p. 100095, 2024.
- [7] J. Omwamba, L. Rotaris, and G. Longo, “An assessment of proximity in the 15-minute city: A systematic literature review,” *Urban Transitions*, p. 100012, 2025.
- [8] E. Papadopoulos, A. Sdoukopoulos, and I. Politis, “Measuring compliance with the 15-minute city concept: State-of-the-art, major components and further requirements,” *Sustainable Cities and Society*, vol. 99, p. 104875, 2023.
- [9] G. Pozoukidou and Z. Chatziyiannaki, “15-minute city: Decomposing the new urban planning eutopia,” *Sustainability*, vol. 13, no. 2, p. 928, 2021.
- [10] A. R. Khavarian-Garmsir, A. Sharifi, and A. Sadeghi, “The 15-minute city: Urban planning and design efforts toward creating sustainable neighborhoods,” *Cities*, vol. 132, p. 104101, 2023.
- [11] T. Abbasov, C. Heine, S. Sabouri, A. Salazar-Miranda, P. Santi, E. Glaeser, and C. Ratti, “The 15-minute city quantified using human mobility data,” *Nature Human Behaviour*, vol. 8, no. 3, pp. 445–455, 2024.
- [12] D. Rhoads, A. Solé-Ribalta, and J. Borge-Holthoefer, “The inclusive 15-minute city: Walkability analysis with sidewalk networks,” *Computers, Environment and Urban Systems*, vol. 100, p. 101936, 2023.
- [13] M. Bruno, H. P. Monteiro Melo, B. Campanelli, and V. Loreto, “A universal framework for inclusive 15-minute cities,” *Nature Cities*, vol. 1, no. 10, pp. 633–641, 2024.
- [14] J. Ramsden and G. Kiss-Haypál, “Company size distribution in different countries,” *Physica A: Statistical Mechanics and its Applications*, vol. 277, no. 1-2, pp. 220–227, 2000.
- [15] R. L. Axtell, “Zipf distribution of u.s. firm sizes,” *Science*, vol. 293, pp. 1818–1820, 2001.
- [16] E. Gaffeo, M. Gallegati, and A. Palestrini, “On the size distribution of firms: Additional evidence from the g7 countries,” *Physica A: Statistical Mechanics and its Applications*, vol. 324, pp. 117–123, 2003.
- [17] X. Gabaix, “Power laws in economics: An introduction,” *Journal of Economic Perspectives*, vol. 30, no. 1, pp. 185–206, 2016.
- [18] T. T. O. Santos and D. O. Cajueiro, “Zipf’s law in the distribution of brazilian firm size,” *arXiv preprint arXiv:2409.09470*, 2024.
- [19] K. S. Sridhar and G. Wan, “Firm location choice in cities: Evidence from china, india, and brazil,” *China Economic Review*, vol. 21, no. 1, pp. 113–122, 2010.
- [20] A. Anas, R. Arnott, and K. A. Small, “Urban spatial structure,” *Journal of Economic Literature*, vol. 36, no. 3, pp. 1426–1464, 1998.
- [21] S. Berroir, H. Mathian, T. Saint-Julien, and L. Sanders, “The role of mobility in the building of metropolitan polycentrism,” in *Modelling Urban Dynamics*, F. Desrosiers and M. Thériault, Eds. ISTE-Wiley, 2011, pp. 1–25.
- [22] A. Bertaud and S. Malpezzi, “The spatial distribution of population in 48 world cities: implications for economies in transition,” 2003.
- [23] F. Le Néchet, “Urban spatial structure, daily mobility and energy consumption: a study of 34 european cities,” *Cybergeo*, no. 580, 2012.
- [24] T. Louail, M. Barthelemy, M. Picornell, R. Herranz, E. Frias-Martinez, and J. J. Ramasco, “From mobile phone data to the spatial structure of cities,” *Scientific Reports*, vol. 4, p. 5276, 2014.
- [25] M. Batty, *The New Science of Cities*. MIT Press, 2013.
- [26] A. Okabe, B. Boots, K. Sugihara, and S. N. Chiu, “Spatial tessellations: concepts and applications of voronoi diagrams,” 2009.
- [27] S. Kirkpatrick, C. D. J. Gelett, and M. P. Vecchi, “Optimization by simulated annealing,” *Science*, vol. 220, no. 4598, pp. 671–680, 1983.
- [28] INSEE, “Près de 60 % des actifs travaillant à paris ne résident pas dans la capitale,” 2022, in French. [Online]. Available: <https://www.insee.fr/fr/statistiques/5057486>
- [29] Greffe du Tribunal de Commerce de Paris, “Atlas économique de paris 2018,” 2018, in French. [Online]. Available: https://www.greffe-tae-paris.fr/uploads/paris/communication/Atlas/Atlas_economique_de_Paris_2018_greffe_tc_Paris_VD.pdf
- [30] INSEE, “Dossier complet: Paris urban unit (2020 definition),” 2023. [Online]. Available: <https://www.insee.fr/fr/statistiques/2011101?geo=UU2020-00851#chiffre-cle-10>
- [31] U.S. Census Bureau, “County business patterns,” 2023. [Online]. Available: <https://www.census.gov/programs-surveys/cbp.html>

Supplementary Information

Why urban heterogeneity limits the 15-minute city

I. EMPIRICAL ANALYSIS: METROPOLITAN STATISTICAL AREAS (US)

We present an empirical analysis of firm-size statistics for U.S. Metropolitan Statistical Areas (MSAs). All datasets are produced by the U.S. Census Bureau. We use the *County Business Patterns* (CBP) release [1], which provides for each MSA: (i) total employment E , (ii) total number of establishments N , and (iii) counts of establishments in discrete employment-size bins. Population estimates for MSAs are taken from Census population estimates [2].

A. Total employment and number of establishments

We first examine how the total number of establishments N varies with total employment E across MSAs. These two aggregates are linked by the mean firm size $\langle m \rangle = E/N$. If the average firm size were approximately constant across MSAs, one would expect a proportionality $N \propto E$. Systematic deviations from linearity may instead reflect changes in the underlying firm-size distribution with metropolitan scale.

Figure S1 shows N as a function of E for all MSAs with strictly positive values, using logarithmic axes. We compare two different fits: (i) a power-law scaling $N = a E^\beta$ obtained from linear regression in log-log space, and (ii) a linear relation constrained to pass through the origin, $N = c E$, corresponding to constant mean firm size. To quantify the strength of the relationship, the figure reports the Pearson correlation coefficient r (computed in log space) and the corresponding goodness-of-fit indicators R^2 . The power-law fit is very close to linear, with an exponent $\simeq 0.93$, and is nearly indistinguishable from a purely linear regression over the observed range. We therefore conclude that the data are consistent with a linear relationship of the form

$$N \simeq \alpha E, \quad (\text{S1})$$

where $1/\alpha$ corresponds to the average number of employees per establishment. In the following, we adopt this linear approximation in both the analytical model and the numerical experiments, using the empirical value $\alpha \simeq 0.06$.

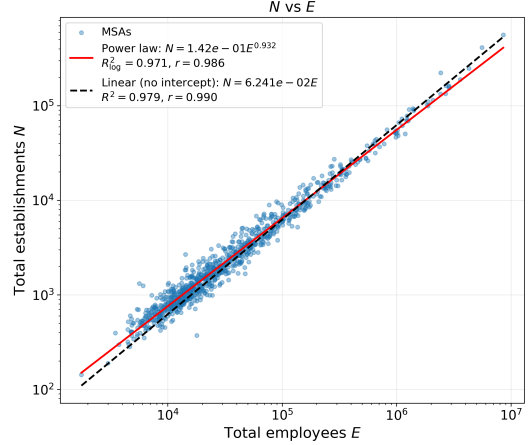


FIG. S1. Total number of establishments N as a function of total employment E across U.S. MSAs. Each point is one MSA (only MSAs with $E > 0$ and $N > 0$ are shown). The solid line is a power-law fit $N = a E^\beta$ obtained from a regression in log-log space. The dashed line is a linear fit constrained to pass through the origin, $N = c E$, which corresponds to constant mean firm size. Both axes are logarithmic; the figure reports correlation and fit-quality diagnostics.

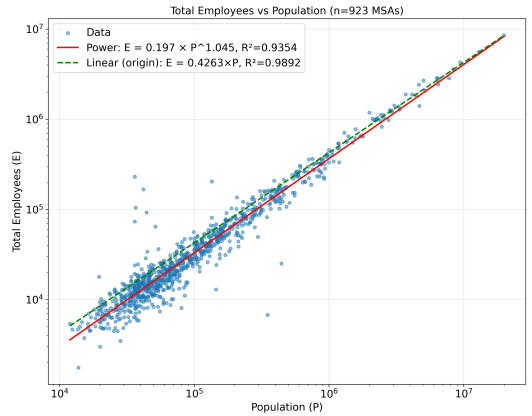


FIG. S2. Total employment E as a function of MSA population P for MSAs with matched population estimates. Each point is one MSA. Axes are shown on logarithmic scales. (Caption to be updated once the final fitting/diagnostic overlays used in the notebook are fixed and exported.)

B. Employment and population

Although we won't use it in this paper, population provides an additional control for metropolitan size. Once MSA populations are matched to the CBP sample, we can analyze how total employment E scales with population P and compare with extensive expectations (e.g. $E \propto P$). Figure S2 reports the resulting relationship. Here

again, the data are consistent with a linear relationship of the form

$$E = \eta P, \quad (\text{S2})$$

with $\eta \simeq 0.43$ for the case of MSAs. The parameter η thus corresponds to the fraction of active workers in the total population.

C. Estimation of the Zipf/Pareto tail exponent from binned CBP data

1. Method

For each Metropolitan Statistical Area (MSA), the County Business Patterns (CBP) dataset reports the number of establishments whose employment size m (number of employees) falls within predefined size classes [1]. Let

$$[a_i, b_i], \quad i = 1, \dots, B,$$

denote the boundaries of the employment-size bins, and let n_i be the corresponding number of establishments in bin i , where B is the total number of bins. All bins are finite except for the top open-ended bin, denoted $[a_B, \infty)$.

In the CBP tables analyzed here, the open-ended bin corresponds to establishments with $m \geq 5000$ employees. The complete set of bins is

$$\begin{aligned} m &< 5, \\ 5 &\leq m \leq 9, \\ 10 &\leq m \leq 19, \\ 20 &\leq m \leq 49, \\ 50 &\leq m \leq 99, \\ 100 &\leq m \leq 249, \\ 250 &\leq m \leq 499, \\ 500 &\leq m \leq 999, \\ 1000 &\leq m \leq 1499, \\ 1500 &\leq m \leq 2499, \\ 2500 &\leq m \leq 4999, \\ m &\geq 5000. \end{aligned} \quad (\text{S3})$$

Empirical firm-size distributions very likely deviate from a power law at small sizes. Accordingly, we do not attempt to model the full distribution $P(m)$ over all m . Instead, we assume that for sufficiently large firm sizes $m \geq m_{\min}$, the distribution follows a Pareto (power-law) form,

$$p(m | m \geq m_{\min}) = C m^{-\nu}, \quad m \geq m_{\min}, \quad (\text{S4})$$

where $\nu > 1$ is the tail exponent and C ensures normalization over the *conditional* support $[m_{\min}, \infty)$.

Crucially, this formulation does *not* impose any as-

sumption on the distribution of firm sizes below m_{\min} . The probability mass below the cutoff, $q \equiv \mathbb{P}(m \geq m_{\min})$, is left unspecified and is estimated empirically from the data. The power-law model thus applies only to the conditional tail distribution $P(m | m \geq m_{\min})$.

The associated Zipf (rank-size) exponent is given by (see e.g. [3])

$$\gamma \equiv \frac{1}{\nu - 1}, \quad (\text{S5})$$

which yields the standard rank-size scaling $m(r) \propto r^{-\gamma}$ used in the main text.

For $\nu \neq 1$, normalization of (S4) implies

$$C = (\nu - 1) m_{\min}^{\nu-1}, \quad \mathbb{P}(m \geq x | m \geq m_{\min}) = \left(\frac{m_{\min}}{x} \right)^{\nu-1}.$$

Hence, for a finite bin $[a_i, b_i]$ with $a_i \geq m_{\min}$ and $b_i < \infty$, the conditional probability mass is

$$P_i(\nu; m_{\min}) = \mathbb{P}(a_i \leq m \leq b_i | m \geq m_{\min}) = \frac{a_i^{1-\nu} - b_i^{1-\nu}}{m_{\min}^{1-\nu}}. \quad (\text{S6})$$

For the open-ended bin $[a_B, \infty)$ with $a_B \geq m_{\min}$,

$$P_\infty(\nu; m_{\min}) = \mathbb{P}(m \geq a_B | m \geq m_{\min}) = \left(\frac{m_{\min}}{a_B} \right)^{\nu-1}. \quad (\text{S7})$$

By construction, the probabilities $\{P_b\}$ sum to unity over the retained tail bins.

For a fixed cutoff m_{\min} , we retain only bins with lower boundary $a_b \geq m_{\min}$ and nonzero counts $n_b > 0$. Let $\mathcal{B}(m_{\min})$ denote this set of tail bins. Conditioned on $m \geq m_{\min}$, the binned counts follow a multinomial distribution with probabilities $\{P_b(\nu; m_{\min})\}$. The corresponding log-likelihood reads

$$\log \mathcal{L}(\nu; m_{\min}) = \sum_{b \in \mathcal{B}(m_{\min})} n_b \log P_b(\nu; m_{\min}), \quad (\text{S8})$$

where P_b is given by Eq. S6 (or Eq. S7 for the last bin). The maximum-likelihood estimate of the tail exponent is

$$\hat{\nu}(m_{\min}) = \arg \max_{\nu > 1} \log \mathcal{L}(\nu; m_{\min}). \quad (\text{S9})$$

In practice, we perform a bounded one-dimensional numerical optimization over $\nu \in [1.1, 6]$ and only attempt a fit when at least two bins remain after thresholding, i.e. $|\mathcal{B}(m_{\min})| \geq 2$. The inferred Zipf exponent then follows from (S5):

$$\hat{\gamma}(m_{\min}) = \frac{1}{\hat{\nu}(m_{\min}) - 1}. \quad (\text{S10})$$

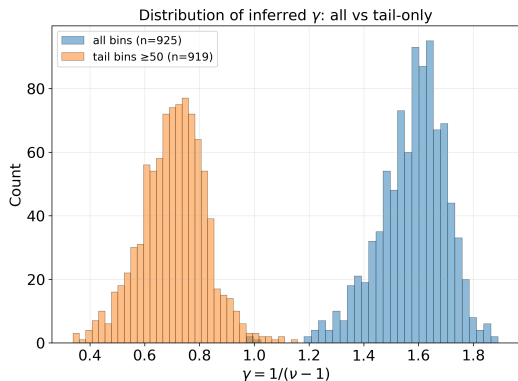


FIG. S3. Distribution of inferred Zipf exponents $\gamma = 1/(\nu - 1)$ across U.S. MSAs. The figure compares estimates obtained using all non-empty bins versus tail-only estimation above a lower cutoff m_{\min} (here $m_{\min} = 50$ employees, i.e. retaining CBP bins with lower boundary $a_b \geq 50$).

2. Empirical results

Using the estimator described above, we compute $\hat{\nu}$ for each MSA and convert it to the corresponding Zipf exponent $\hat{\gamma} = 1/(\hat{\nu} - 1)$. Since the Pareto assumption is intended to hold only for sufficiently large establishments, we focus on a tail threshold $m_{\min} = 50$ employees (unless otherwise stated) and report the resulting distribution of exponents across MSAs.

Figure S3 compares the inferred Zipf exponents obtained (i) by fitting all non-empty bins and (ii) by restricting the estimation to tail bins with lower boundary $a_b \geq m_{\min}$. The two procedures yield markedly different results. When all bins are included, the distribution is narrowly peaked around $\gamma_{\text{all}} \simeq 1.6$ (corresponding to $\nu_{\text{all}} \simeq 1.64$), with relatively small dispersion across MSAs. In contrast, tail-only estimation produces a substantially smaller exponent, with mean $\gamma_{\text{tail}} \simeq 0.71$ (corresponding to $\nu_{\text{tail}} \simeq 2.46$), and a noticeably broader distribution.

To assess the robustness of the inferred tail exponent, we repeated the estimation procedure for different choices of the lower cutoff m_{\min} . In addition to the baseline value $m_{\min} = 50$, we considered thresholds $m_{\min} = 30$ and $m_{\min} = 100$ employees, corresponding to progressively looser and stricter definitions of the tail.

As expected, the inferred exponent exhibits a systematic dependence on m_{\min} . For $m_{\min} = 30$, the average tail exponent across MSAs is $\langle \gamma_{\text{tail}} \rangle \simeq 1.25$ ($\langle \nu_{\text{tail}} \rangle \simeq 1.81$), reflecting residual influence from the upper part of the distribution body. Increasing the cutoff to $m_{\min} = 50$ yields $\langle \gamma_{\text{tail}} \rangle \simeq 0.71$ ($\langle \nu_{\text{tail}} \rangle \simeq 2.46$), while a more conservative choice $m_{\min} = 100$ further lowers the exponent to $\langle \gamma_{\text{tail}} \rangle \simeq 0.65$ ($\langle \nu_{\text{tail}} \rangle \simeq 2.60$), at the cost of reducing the number of MSAs with sufficient tail data.

This monotonic decrease of γ_{tail} with increasing m_{\min} is consistent with a gradual crossover from the body of the firm-size distribution to its asymptotic tail. Importantly,

once the cutoff is chosen within a reasonable range ($m_{\min} \gtrsim 50$), the inferred exponents stabilize in a narrow interval $\gamma_{\text{tail}} \approx 0.6\text{--}0.7$, indicating a robust heavy-tailed regime for large establishments. The qualitative conclusions of the paper are insensitive to the precise choice of m_{\min} within this range.

This systematic shift reflects the fact that the lower part of the firm-size distribution is probably not well described by a pure power law. Including small-size bins effectively forces the fit to compromise between the body and the tail, resulting in artificially shallow Pareto exponents. Restricting the estimation to the tail isolates the scaling behavior of large establishments, which is the regime of interest for aggregate employment concentration and commuting constraints. Importantly, the tail-only exponents remain remarkably stable across MSAs despite large variations in total employment ($E \simeq 1.4 \times 10^5$ on average, with standard deviation exceeding the mean by a factor ~ 3.6). This suggests that the heavy-tailed nature of firm sizes is a robust, city-independent feature of urban economies, while the body of the distribution primarily reflects local institutional and sectoral effects.

Throughout the main text, we therefore rely on tail-based estimates $\hat{\gamma}_{\text{tail}}$, which provide a more faithful characterization of the asymptotic firm-size heterogeneity relevant for proximity and accessibility constraints.

3. Prediction of the largest establishment size

Given the total employment E , the total number of establishments N_{est} , and an estimated tail exponent $\hat{\gamma}$, the model yields a theoretical prediction for the size of the largest establishment, denoted m_1^{theo} . This prediction follows from the normalization of the associated rank-size relation. Assuming a Zipf law for establishment sizes,

$$m(r) = m_1 r^{-\gamma}, \quad r = 1, \dots, N_{\text{est}}, \quad (\text{S11})$$

the total employment satisfies

$$E = \sum_{r=1}^{N_{\text{est}}} m(r) = m_1 \sum_{r=1}^{N_{\text{est}}} r^{-\gamma} \equiv m_1 H_{N_{\text{est}}}(\gamma), \quad (\text{S12})$$

where $H_N(\gamma) = \sum_{r=1}^N r^{-\gamma}$ is the generalized harmonic number. This immediately yields the theoretical prediction

$$m_1^{\text{theo}} = \frac{E}{H_{N_{\text{est}}}(\hat{\gamma})}. \quad (\text{S13})$$

We compare this theoretical prediction to an empirical proxy extracted from the CBP binning. For each MSA, the largest non-empty employment bin provides lower and upper bounds ($m_{1,\text{low}}, m_{1,\text{high}}$) on the size of the largest observed establishment. Because the precise firm size within the top bin is unknown, this compari-

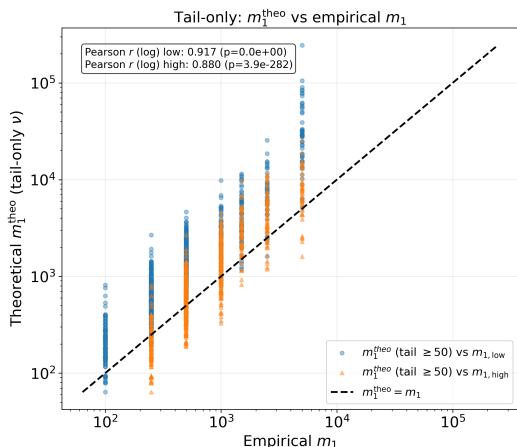


FIG. S4. Tail-only theory–data comparison for the largest establishment size. For each MSA, m_1^{theo} is computed using the tail-based exponent estimate (retaining bins with $a_b \geq m_{\min}$, here $m_{\min} = 50$). The empirical largest-establishment size is bracketed by the lower and upper boundaries of the largest non-empty CBP bin, $(m_{1,\text{low}}, m_{1,\text{high}})$. The dashed line indicates $m_1^{\text{theo}} = m_1$.

son is necessarily approximate and should be interpreted within these bounds.

We focus on the tail-based exponent estimate (with cutoff $m_{\min} = 50$), which is consistent with the modeling assumption that the Pareto form applies only at large employment sizes. Figure S4 shows the comparison between the theoretical prediction m_1^{theo} and the empirical bounds $(m_{1,\text{low}}, m_{1,\text{high}})$ across MSAs. The dashed diagonal indicates perfect agreement, $m_1^{\text{theo}} = m_1$.

Despite the coarse binning of the empirical data, the theoretical predictions fall systematically within, or close to, the empirical bounds. To quantify this agreement, we compute Pearson correlation coefficients between $\log m_1^{\text{theo}}$ and $\log m_{1,\text{low}}$ (and similarly for $m_{1,\text{high}}$ where available). For the lower-bound comparison, we find a strong correlation ($r \simeq 0.92$), indicating that the model captures the cross-MSA variability in the size of the largest establishment remarkably well. This agreement provides an independent consistency check on both the tail-based estimation of γ and the internal coherence of the model.

II. THEORETICAL ANALYSIS: MODEL DEFINITION AND FEASIBILITY BOUNDS

A. Model definition

We consider an idealized city of characteristic radius R and total population P , total number of employees E , with residents uniformly distributed in space unless stated otherwise. Employment is provided by N firms, whose sizes are heterogeneous and ranked by decreasing employment. Firm sizes follow a Zipf distribution, such that the firm of rank r employs $m_r \propto r^{-\gamma}$ workers,

where the exponent γ controls the degree of economic inequality: $\gamma = 0$ corresponds to homogeneous firms, while larger values of γ indicate increasingly concentrated employment in a small number of large firms.

More precisely, the idealized city occupies a disk $\Omega = \{\mathbf{r} \in \mathbb{R}^2 : \|\mathbf{r}\| \leq R\}$ with total employment (and population, assuming full employment) E . Residents are distributed with a radially symmetric density $\rho(r)$, normalized as

$$\int_{\Omega} \rho(\mathbf{r}) d^2\mathbf{r} = E. \quad (\text{S14})$$

Unless stated otherwise, commuting distances are Euclidean.

Employment is provided by N establishments (“firms”), indexed by decreasing size (rank) $r = 1, \dots, N$. Establishment sizes follow a Zipf law

$$m_r = \frac{m_1}{r^\gamma}, \quad r = 1, \dots, N, \quad (\text{S15})$$

where $\gamma \geq 0$ controls heterogeneity. The normalization $\sum_{r=1}^N m_r = E$ implies

$$m_1 = \frac{E}{H_N^{(\gamma)}}, \quad H_N^{(\gamma)} = \sum_{r=1}^N \frac{1}{r^\gamma}. \quad (\text{S16})$$

The behavior of $H_N^{(\gamma)}$ for large N depends on the value of γ :

$$H_N^{(\gamma)} \sim \begin{cases} \frac{N^{1-\gamma}}{1-\gamma} & \text{for } \gamma < 1 \\ \log N + \gamma_e & \text{for } \gamma = 1 \\ \zeta(\gamma) + \mathcal{O}(N^{1-\gamma}) & \text{for } \gamma > 1 \end{cases} \quad (\text{S17})$$

Empirically, the number of establishments scales approximately linearly with total employment:

$$N = \alpha E, \quad (\text{S18})$$

with $\alpha \approx 0.06$ in our datasets (mean establishment size $\simeq 1/\alpha$).

B. Feasibility problem and definition of ℓ_{\max}

The x-minute city constraint requires that every worker can reach their assigned firm within travel distance ℓ . The theoretical minimum ℓ_{theo} is determined by the largest firm, which must capture a fraction $1/H_N^{(\gamma)}$ of the total population within its catchment area.

Let $\mathbf{x}_r \in \Omega$ be the location of establishment r . A feasible assignment at commuting threshold L_0 is a partition of the population into disjoint catchment regions $A_r \subset \Omega$ such that

$$\int_{A_r} \rho(\mathbf{r}) d^2\mathbf{r} = m_r, \quad \sup_{\mathbf{r} \in A_r} \|\mathbf{r} - \mathbf{x}_r\| \leq L_0 \quad \forall r, \quad (\text{S19})$$

and $\cup_{r=1}^N A_r = \Omega$. For a given configuration, the maximum commute distance is

$$\ell_{\max} = \max_r \sup_{\mathbf{r} \in A_r} \|\mathbf{r} - \mathbf{x}_r\|. \quad (\text{S20})$$

The central question is whether there exist locations $\{\mathbf{x}_r\}$ and an assignment $\{A_r\}$ such that $\ell_{\max} \leq L_0$.

C. A general lower bound from the largest establishment

A necessary condition for feasibility follows from the largest establishment. Even with optimal placement of establishment $r = 1$ at the density maximum, its catchment must contain $m_1 = E/H_N^{(\gamma)}$ workers within radius L_0 . Define the *cumulative population fraction* within distance ℓ of the optimal point (by symmetry, the center for the radial models considered here):

$$F(\ell) = \frac{1}{E} \int_{\|\mathbf{r}\| \leq \ell} \rho(\mathbf{r}) d^2 \mathbf{r}. \quad (\text{S21})$$

Then feasibility requires

$$F(L_0) \geq \frac{m_1}{E} = \frac{1}{H_N^{(\gamma)}}. \quad (\text{S22})$$

Equivalently, a *theoretical feasibility bound* is obtained by solving

$$\boxed{F(L_0^*) = \frac{1}{H_N^{(\gamma)}}} \quad \Rightarrow \quad L_0 \geq L_0^*. \quad (\text{S23})$$

This bound is *necessary* (but not sufficient): even if the largest establishment can be served within L_0^* , other capacity constraints may still force a larger L_0 .

A complementary (more local) necessary bound uses only the maximum density $\rho_{\max} = \max_{\mathbf{r} \in \Omega} \rho(\mathbf{r})$:

$$m_1 \leq \int_{\|\mathbf{r}\| \leq L_0} \rho(\mathbf{r}) d^2 \mathbf{r} \leq \rho_{\max} \pi L_0^2 \quad \Rightarrow \quad L_0 \geq \sqrt{\frac{m_1}{\pi \rho_{\max}}}. \quad (\text{S24})$$

For radially decreasing densities, the bound (S23) is sharper.

D. Uniform density

We first consider the case of a uniform employment density over a disk of radius R , i.e.

$$\rho(r) = \frac{E}{\pi R^2}.$$

In this case, Eq. (S21) yields

$$F(\ell) = \left(\frac{\ell}{R}\right)^2, \quad 0 \leq \ell \leq R, \quad (\text{S25})$$

which simply corresponds to the fraction of area contained within a disk of radius ℓ .

Inserting this expression into Eq. (S23) and solving for the characteristic distance yields

$$\boxed{L_0^{*(\text{unif})} = \frac{R}{\sqrt{H_N(\gamma)}}}, \quad (\text{S26})$$

where $H_N(\gamma) = \sum_{r=1}^N r^{-\gamma}$ denotes the generalized harmonic number associated with the Zipf exponent γ .

Equation (S26) highlights how firm-size heterogeneity controls the minimal characteristic distance through $H_N(\gamma)$. Several limiting cases are of particular interest:

- **Homogeneous establishments** ($\gamma = 0$). In this case $H_N(0) = N$, leading to

$$L_0^{*(\text{unif})} = \frac{R}{\sqrt{N}},$$

which corresponds to the typical spacing of a space-filling tessellation (e.g. optimal hexagonal packing).

- **Zipf regime** ($\gamma = 1$). The harmonic sum diverges logarithmically, $H_N(1) \simeq \ln N$, yielding

$$L_0^{*(\text{unif})} \sim \frac{R}{\sqrt{\ln N}}.$$

- **Strong heterogeneity** ($\gamma > 1$). The harmonic sum converges to the Riemann zeta function, $H_N(\gamma) \rightarrow \zeta(\gamma)$ as $N \rightarrow \infty$, implying

$$L_0^{*(\text{unif})} \rightarrow \frac{R}{\sqrt{\zeta(\gamma)}}.$$

In this regime, the distance threshold becomes independent of the number of establishments and is controlled solely by the degree of heterogeneity.

E. Exponential radial density

For centralized cities, we consider an exponential density (a standard assumption for monocentric cities, see for example the original work [4])

$$\rho(r) = \rho_0 e^{-r/R_d}, \quad r \geq 0, \quad (\text{S27})$$

with decay length R_d and an outer cutoff $R_{\text{disk}} \gg R_d$. In the limit $R_{\text{disk}} \rightarrow \infty$, normalization gives $E = 2\pi\rho_0 R_d^2$

and

$$F(\ell) = 1 - \left(1 + \frac{\ell}{R_d}\right) \exp\left(-\frac{\ell}{R_d}\right). \quad (\text{S28})$$

The bound (S23) becomes

$$1 - (1+x)e^{-x} = \frac{1}{H_N^{(\gamma)}}, \quad x = \frac{L_0^{*(\text{exp})}}{R_d}. \quad (\text{S29})$$

Equivalently,

$$(1+x)e^{-x} = 1 - \frac{1}{H_N^{(\gamma)}}. \quad (\text{S30})$$

This equation can be solved numerically for x . An explicit closed form uses the Lambert W function:

$$x = -1 - W\left(-\frac{1 - \frac{1}{H_N^{(\gamma)}}}{e}\right), \quad L_0^{*(\text{exp})} = R_d x. \quad (\text{S31})$$

For small radii ($x \ll 1$), Eq. (S28) gives $F(\ell) \simeq x^2/2$, so the exponential case behaves as

$$L_0^{*(\text{exp})} \simeq R_d \sqrt{\frac{2}{H_N^{(\gamma)}}} \quad (\text{when } 1/H_N^{(\gamma)} \ll 1). \quad (\text{S32})$$

Compared at fixed $H_N^{(\gamma)}$, the required L_0^* depends on the chosen macroscopic scale (R vs R_d); thus, uniform vs exponential should be compared using consistent city-size conventions (e.g., fixing the same outer radius or the same mean density).

F. Interpretation

Equations (S23)–(S31) show that firm-size inequality enters the feasibility condition only through the fraction $m_1/E = 1/H_N^{(\gamma)}$ that must be served by the largest establishment. For $\gamma < 1$ and $N = \alpha E$, one has $H_N^{(\gamma)} \sim N^{1-\gamma}/(1-\gamma)$, hence $m_1 \sim E/N^{1-\gamma} \propto E^\gamma$, so the constraint induced by the head of the distribution strengthens with system size.

Summary Table:

Property	Uniform Density	Exponential Density
Density profile	$\rho(r) = \rho_0$	$\rho(r) = \rho_0 e^{-r/R}$
Weight function	$F(x) = x^2$	$F(x) = 1 - (1+x)e^{-x}$
Feasibility condition	$(\ell/R)^2 = 1/H_N$	$(1 + \ell/R)e^{-\ell/R} = 1 - 1/H_N$
Theoretical bound	$\ell = R/\sqrt{H_N}$	Solve numerically
Small ℓ behavior	$\ell \propto 1/\sqrt{H_N}$	$\ell \propto \sqrt{2/H_N}$

TABLE I. Comparison of theoretical bounds for uniform and exponential population densities.

III. DEPENDENCE ON CAPACITY TOLERANCE

Our model allows firms to operate with flexible capacity: firm i with target size m_i can employ between $(1-\delta)m_i$ and $(1+\delta)m_i$ workers, where $\delta \in [0, 1]$ is the tolerance parameter. This flexibility captures realistic features of labor markets, including part-time employment, seasonal fluctuations, and firms operating below maximum capacity. Here we examine how δ affects the optimized accessibility ratio across different firm-size distributions parametrized by the Zipf exponent γ .

The theoretical lower bound $\ell_{\text{theo}}^{(0)} = R/\sqrt{H_N^{(\gamma)}}$ assumes *strict* capacity constraints ($\delta = 0$), where each firm must employ exactly m_i workers. With flexible capacity, the constraint is relaxed: the largest firm need only recruit its *minimum* required workforce $(1-\delta)m_1 = (1-\delta)P/H_N^{(\gamma)}$. When optimally placed at the population density maximum, this requirement becomes:

$$W\left(\frac{\ell}{R}\right) \geq \frac{1-\delta}{H_N^{(\gamma)}}, \quad (\text{S33})$$

where $W(x)$ is the cumulative population fraction within dimensionless radius x . The flexibility-corrected theoretical bound is therefore:

$$\ell_{\text{theo}}^{(\delta)} = R \cdot W^{-1}\left(\frac{1-\delta}{H_N^{(\gamma)}}\right). \quad (\text{S34})$$

For uniform population density, $W(x) = x^2$, yielding the explicit formula:

$$\ell_{\text{theo}}^{(\delta)} = R \sqrt{\frac{1-\delta}{H_N^{(\gamma)}}} = \sqrt{1-\delta} \cdot \ell_{\text{theo}}^{(0)}. \quad (\text{S35})$$

For $\delta = 30\%$, this gives $\ell_{\text{theo}}^{(0.3)} = \sqrt{0.7} \ell_{\text{theo}}^{(0)} \approx 0.84 \ell_{\text{theo}}^{(0)}$, meaning that a 30% flexibility margin reduces the minimum feasible travel distance by approximately 16% in the uniform-density case ($1 - \sqrt{0.7} \approx 0.16$). For exponential population density, $W(x) = 1 - (1+x)e^{-x}$, and Eq. (S34) must be inverted numerically.

IV. NUMERICAL METHOD

A. General approach

The x -minute city feasibility problem can be formulated as:

Given parameters $(E, R, N, \gamma, m_{\min})$, find firm locations $\{\mathbf{x}_j\}_{j=1}^N$ and an assignment $c: \{1, \dots, E\} \rightarrow \{1, \dots, N\}$ such that:

1. Each firm j is assigned exactly m_j employees.

2. The maximum commute distance $\ell_{\max} \leq L_0$.

Equivalently, we seek to minimize ℓ_{\max} over firm locations:

$$\ell_{\max}^* = \min_{\{\mathbf{x}_j\}} \left[\min_c \max_i d(i, c(i)) \right], \quad (\text{S36})$$

subject to capacity constraints. The feasibility threshold L_0^{\min} is the smallest L_0 for which a valid configuration exists.

1. Goal and outputs

The numerical objective is to estimate, for given parameters (E, R, γ, α) and a chosen population density model, the minimal achievable maximum commuting distance

$$\ell_{\max}^*(\gamma) = \min_{\{\mathbf{x}_r\} \subset \Omega} \left[\min_{\{A_r\}} \max_r \sup_{\mathbf{r} \in A_r} \|\mathbf{r} - \mathbf{x}_r\| \right], \quad (\text{S37})$$

under the capacity constraints $\int_{A_r} \rho(\mathbf{r}) d^2\mathbf{r} = m_r$. We compare $\ell_{\max}^*(\gamma)$ to the theoretical lower bound $\ell_{\text{theo}}(\gamma)$ from Sec. S23, and we build feasibility curves (or “phase diagrams”) in the (γ, L_0) plane by declaring the system feasible whenever $\ell_{\max}^*(\gamma) \leq L_0$.

2. Discretization of the population

We represent the population by E points $\{\mathbf{r}_i\}_{i=1}^E$ sampled independently from the prescribed density $\rho(r)$ within the disk of radius R . In practice, we use moderate sizes (typically $E \sim 10^4$) to keep the optimization tractable, and we verify robustness by repeating runs with different random seeds.

B. Establishment sizes and empirical scaling

$$N = \alpha E$$

For each run and each Zipf exponent γ , we set the number of establishments via

$$N = \lfloor \alpha E \rfloor, \quad (\text{S38})$$

and define capacities $\{m_r\}_{r=1}^N$ by the Zipf law (S15) with normalization (S16). Capacities are then converted to integers that sum exactly to E by rounding and distributing the remainder. Optionally, we allow a tolerance window $m_r(1 \pm \delta)$ to account for finite-sampling fluctuations in the discretized population (we report δ explicitly whenever used).

1. Assignment subproblem

Given establishment positions $\{\mathbf{x}_r\}$ and capacities $\{m_r\}$, we assign each individual to one establishment such that (i) capacity constraints are satisfied and (ii) distances are short. Exact minimization of ℓ_{\max} under capacities is computationally expensive; we therefore use a fast greedy procedure that iterates through individuals and assigns each one to the nearest establishment with remaining capacity, querying all establishments (via pairwise distances) to avoid artificial “fallback” artifacts. For each configuration we record the resulting ℓ_{\max} .

2. Optimization of establishment locations

To minimize the maximum commuting distance ℓ_{\max} over establishment locations, we use a simulated annealing (SA) heuristic, which is well suited for high-dimensional problems with many local minima. The objective function is defined as the maximum Euclidean distance between any worker and the establishment to which they are assigned, given the firm capacities and the current spatial configuration.

Each SA run starts from an initial configuration in which establishments are placed on a regular, approximately hexagonal lattice within the disk of radius R , ensuring a homogeneous initial coverage of space. At each Monte Carlo step, a single establishment is selected at random and displaced by a small random vector drawn from an isotropic distribution with a fixed step size. Proposed moves that place the establishment outside the disk are rejected.

For a proposed displacement, the change in the objective function, $\Delta\ell_{\max}$, is computed by recomputing the worker–establishment assignment and the resulting maximum commuting distance. Moves that decrease ℓ_{\max} are always accepted, while moves that increase it are accepted with probability $\exp(-\Delta\ell_{\max}/T)$, where T is the current annealing temperature (Metropolis criterion). The temperature is gradually reduced according to a prescribed cooling schedule until the system becomes effectively frozen and no further improvements are observed.

To reduce sensitivity to initial conditions and stochastic fluctuations, the SA procedure is repeated for multiple independent initial seeds and random number streams. Among all runs, we retain the configuration yielding the smallest value of ℓ_{\max} , which is reported as the optimized solution for the given parameter set.

3. Capacity tolerance δ and feasibility relaxation

In the discrete formulation, each establishment r must be assigned exactly m_r workers, where the target capacities $\{m_r\}$ follow the Zipf law (Eq. (S15)) and are converted to integers so that $\sum_{r=1}^N m_r = E$. For a fixed set of establishment locations $\{\mathbf{x}_r\}$, enforcing the strict

capacity constraints can lead to artificially large ℓ_{\max} in finite samples: even when a “nearly feasible” spatial configuration exists, a small mismatch between local worker availability and discrete integer capacities can force some individuals to be assigned far away to satisfy the exact counts.

To control for this finite-size/discretization effect, we introduce a *capacity tolerance* parameter $\delta \geq 0$ that relaxes the hard upper bound on the number of workers that an establishment can accept. Concretely, in the assignment step we replace the capacity constraint

$$n_r \leq m_r \quad (\text{S39})$$

by

$$n_r \leq m_r^{\max}(\delta) \equiv \lceil (1 + \delta) m_r \rceil, \quad (\text{S40})$$

where n_r is the number of workers assigned to establishment r and $\lceil \cdot \rceil$ denotes the ceiling function. The parameter δ therefore controls the allowed relative *overflow* of each establishment, with $\delta = 0$ recovering strict capacities. Because the integer rounding in Eq. (S40) can change the total available capacity, we ensure that the relaxed total capacity is at least E (otherwise no complete assignment can exist); in practice we increase all m_r^{\max} by a common multiplicative factor of order $1 + \varepsilon$ whenever $\sum_r m_r^{\max}(\delta) < E$.

Operationally, we use δ only during the assignment subproblem: given $\{\mathbf{x}_r\}$, each worker is greedily assigned to the nearest establishment with remaining relaxed capacity, and the resulting maximum distance defines ℓ_{\max} for that configuration. Simulated annealing then minimizes this relaxed objective over establishment locations.

The tolerance δ has two interpretations: (i) it reduces spurious infeasibility that originates from discrete sampling of a continuous density field and integer capacities; and (ii) it can be viewed as a coarse-grained representation of real-world flexibility, where establishments can absorb modest deviations from target headcounts (through temporary overstaffing, part-time work, multi-site allocation, or measurement noise in the empirical size distribution).

In the main numerical results we report $\ell_{\max}^*(\gamma, \delta)$ for a fixed δ (typically $\delta \simeq 0.3$) and show that qualitative trends with γ are robust. Importantly, because $\delta > 0$ relaxes constraints, $\ell_{\max}^*(\gamma, \delta)$ is decreasing with δ ; hence the strict-capacity case $\delta = 0$ provides the most conservative feasibility assessment, while $\delta > 0$ yields a lower estimate of realistic feasibility when moderate capacity fluctuations are allowed.

4. Numerical Approach: Simulated Annealing

We employ simulated annealing to optimize firm locations [5]. The algorithm proceeds as follows:

Algorithm 1: Simulated Annealing for Firm Location Optimization

Input: Initial temperature T_0 , cooling rate $\alpha \approx 0.95$, minimum temperature T_{\min}
Output: Optimized positions $\{\mathbf{x}_j\}$ and ℓ_{\max}^*
Initialize random firm positions $\{\mathbf{x}_j\}$ within the disk;
 $T \leftarrow T_0$;
while $T > T_{\min}$ **do**
 for $k = 1$ **to** n_{steps} **do**
 Perturb one firm position: $\mathbf{x}_j \leftarrow \mathbf{x}_j + \delta$;
 Compute assignment c (nearest-firm or capacitated);
 Compute new cost $\mathcal{E}' = \ell_{\max}$;
 $\Delta\mathcal{E} \leftarrow \mathcal{E}' - \mathcal{E}$;
 if $\Delta\mathcal{E} < 0$ **or** $\text{rand}() < e^{-\Delta\mathcal{E}/T}$ **then**
 Accept move;
 else
 Reject move;
 end
 end
 $T \leftarrow \alpha T$;
end
return optimized positions $\{\mathbf{x}_j\}$ and ℓ_{\max}^* ;

The primary cost function is the maximum commute distance:

$$\mathcal{E} = \ell_{\max} = \max_i d(i, c(i)). \quad (\text{S41})$$

To map the feasibility landscape, we perform a systematic scan:

1. For each $\gamma \in [0.5, 2.0]$ (discretized)
2. Run simulated annealing to find $\ell_{\max}^*(N, \gamma)$
3. Record $(N, \gamma, \ell_{\max}^*, \bar{\ell}^*)$

V. CASE STUDY: PARIS

In this section, we detail the estimation of the firm-size exponent γ used in the Paris case study. Direct establishment-size data for the administrative city of Paris are not available at a sufficiently fine resolution. We therefore rely on publicly available data for the Paris urban area [6, 7], which provides the closest empirical proxy for the distribution of economic activity at this scale.

The dataset reports the number of establishments grouped into four employment-size classes: 1–9, 10–19, 20–49, and 50 or more employees. To estimate the exponent γ , we assume that firm sizes follow a rank-size (Zipf-like) distribution,

$$m(r) \sim r^{-\gamma}, \quad (\text{S42})$$

which implies a complementary cumulative distribution

of the form $P(m \geq x) \sim x^{-1/\gamma}$. Under this assumption, the expected fraction of establishments in each size class can be computed analytically. The exponent γ is then estimated by fitting these predicted fractions to the empirical bin counts using a multinomial likelihood (see section I.C).

Figure S5 compares the empirical employment-size bins with the best-fit theoretical distribution. The fitted value $\hat{\gamma} \simeq 1.38$ reflects the strong heterogeneity of firm sizes in the Paris metropolitan area, with a large number of small establishments coexisting with a long tail of large employers. Because the data are coarsely binned, this estimate should be interpreted as an effective exponent rather than a precise universal value. For this reason, γ is treated as a control parameter in the main analysis, and a broad range of values is explored to assess the robustness of the feasibility constraints on proximity.

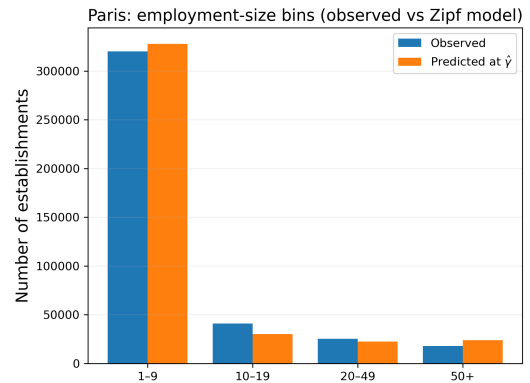


FIG. S5. Empirical employment-size bins for the Paris urban area compared with a rank-size model fitted with exponent $\hat{\gamma} \simeq 1.38$. Bars show the number of establishments in four employment-size classes (1–9, 10–19, 20–49, and 50+ employees), using INSEE data. The fitted model captures the pronounced heterogeneity of firm sizes despite the coarse binning.

-
- [1] U.S. Census Bureau, “County business patterns,” 2023. [Online]. Available: <https://www.census.gov/programs-surveys/cbp.html>
- [2] —, “Metropolitan area population totals: 2020–2023,” <https://www2.census.gov/programs-surveys/popest/tables/2020-2023/metro/totals/>, 2023, accessed: 2026-03-12.
- [3] L. A. Adamic, “Zipf, power-laws, and pareto: A ranking tutorial,” Palo Alto, CA, 2000. [Online]. Available: <https://blogimages.bloggen.be/stijfreter/attach/12750.pdf>
- [4] C. Clark, “Urban population densities,” *Journal of the Royal Statistical Society. Series A (General)*, vol. 114, no. 4, pp. 490–496, 1951.
- [5] S. Kirkpatrick, C. D. J. Gelatt, and M. P. Vecchi, “Optimization by simulated annealing,” *Science*, vol. 220, no. 4598, pp. 671–680, 1983.
- [6] INSEE, “Près de 60 % des actifs travaillant à paris ne résident pas dans la capitale,” 2022, in French. [Online]. Available: <https://www.insee.fr/fr/statistiques/5057486>
- [7] —, “Dossier complet: Paris urban unit (2020 definition),” 2023. [Online]. Available: <https://www.insee.fr/fr/statistiques/2011101?geo=UU2020-00851#chiffre-cle-10>